

The Structural Basis of Hammerhead Ribozyme Self-Cleavage

James B. Murray,* Daniel P. Terwey,* Lara Maloney,† Alexander Karpeisky,† Nassim Usman,† Leonid Beigelman,† and William G. Scott**‡

*Department of Chemistry

Indiana University

Bloomington, Indiana 47405

†Ribozyme Pharmaceuticals Inc.

2950 Wilderness Place

Boulder, Colorado 80301

Summary

We have captured an 8.7 Å conformational change that takes place in the cleavage site of the hammerhead ribozyme during self-cleavage, using X-ray crystallography combined with physical and chemical trapping techniques. This rearrangement brings the hammerhead ribozyme from the ground state into a conformation that is poised to form the transition state geometry required for hammerhead RNA self-cleavage. Use of a 5'-C-methylated ribose adjacent to the cleavage site permits this ordinarily transient conformational change to be kinetically trapped and observed crystallographically after initiating the hammerhead ribozyme reaction in the crystal. Cleavage of the corresponding unmodified hammerhead ribozyme in the crystal under otherwise identical conditions is faster than in solution, indicating that we have indeed trapped a catalytically relevant intermediate form of this RNA enzyme.

Introduction

The discovery that RNA can be an enzyme (Guerrier-Takada et al., 1983; Zaug and Cech, 1986) impels us to answer the question of how such enzymes, or ribozymes, work. Perhaps the simplest and best-characterized ribozyme is the hammerhead ribozyme. Its small size, thoroughly investigated cleavage chemistry, known crystal structure, and its biological as well as potential medical relevance make the hammerhead ribozyme particularly well-suited for biophysical investigations. The hammerhead ribozyme is therefore the ribozyme most likely to enable us to begin to answer the question of how ribozymes actually work.

The hammerhead ribozyme is derived (Uhlenbeck, 1987) from several self-cleaving satellite virus RNAs that replicate via a rolling circle mechanism (Symons, 1992). Extensive biochemical experiments (reviewed in McKay, 1996, and in Thomson et al., 1996) and structural investigations (Pley et al., 1994; Scott et al., 1995, 1996) have yielded a fairly coherent framework for understanding the hammerhead ribozyme. The hammerhead ribozyme is believed to require one or more divalent cations either for folding or catalytic activity under standard (low ionic strength) reaction conditions (Dahm and Uhlenbeck,

1991; Dahm et al., 1993), and it cleaves itself with high specificity with a typical turnover rate of about 0.1–1 per min (depending upon sequence), yielding 5'-OH and 2',3'-cyclic phosphate termini. The log of the rate of hammerhead RNA cleavage tends to increase linearly with pH in the range of about 5–9, allowing the use of pH as a controlling variable in cleavage reaction studies.

We are investigating the mechanism of RNA catalysis using X-ray crystallography. The previous crystal structures of the hammerhead ribozyme ground state conformation (Pley et al., 1994; Scott et al., 1995, 1996) have shown the cleavage site phosphate to be in the standard helical conformation, a geometry maximally incompatible (Brown et al., 1985; McKay, 1996; Scott and Klug, 1996) with the known in-line attack mechanism (van Tol et al., 1990; Koizumi and Ohtsuka, 1991; Slim and Gait, 1991). Therefore, it has been proposed that a conformational change must take place prior to cleavage, allowing an in-line transition state geometry to form (Pley et al., 1994; Scott et al., 1995, 1996; McKay, 1996; Scott and Klug, 1996). We are continuing our crystallographic investigations with the aim of understanding the nature of the conformational change required for hammerhead ribozyme self-cleavage.

In previously reported experiments using crystals of an unmodified hammerhead ribozyme, we tested the biochemical relevance of the hammerhead RNA crystal structures by demonstrating cleavage activity in the crystal (on the order of 0.5/min). We also obtained crystal structures of two states of the uncleaved hammerhead ribozyme (Scott et al., 1996). The first structure was identical to that of the previously determined "ground state" structure of the inactivated hammerhead ribozyme. The second structure was that of a flash-frozen "early" conformational intermediate that presumably exists only transiently in the crystal prior to cleavage, unless captured by crystallographic freeze-trapping techniques (Moffat and Henderson, 1995). The 3 Å movement of the scissile phosphate in this early intermediate encouraged us to propose a mechanism for the hammerhead ribozyme cleavage reaction, invoking an *unobserved* more substantial movement of the scissile phosphate toward a conformation compatible with in-line attack. This crucial "later" (and more chemically relevant) intermediate structure has, however, continued to elude capture using the unmodified hammerhead ribozyme crystals.

To trap the structure of a later hammerhead ribozyme intermediate, we synthesized a modification of the hammerhead ribozyme that creates a "kinetic bottleneck" at the final or bond-breaking point on the reaction pathway. The idea for using such a modification was based upon the success of an analogous experiment with isocitrate dehydrogenase, in which active site modifications allowed two intermediate structures each to accumulate in the crystal with artificially long life spans, enabling their observation using time-resolved crystallographic techniques (Bolduc et al., 1995).

By synthesizing a hammerhead ribozyme of the same

‡ To whom correspondence should be addressed.

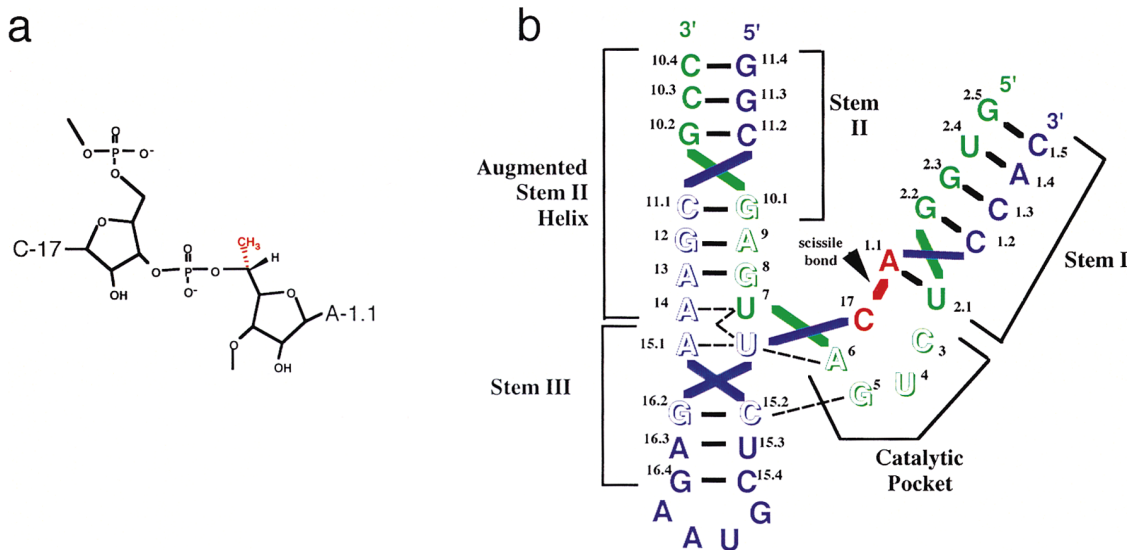


Figure 1. The Cleavage Site Modification and Sequence of the Crystallized Hammerhead Ribozyme

(a) The kinetic bottleneck modification adjacent to the cleavage site. Schematic diagram of the C-17—A-1.1 ribonucleotide backbone depicting the *tallo*-5'-C-methyl-modified-ribose at the cleavage site in red. This methyl group, added adjacent to the 5'-oxygen leaving group of the reaction, creates a kinetic bottleneck at the scissile bond-cleavage stage of the hammerhead RNA cleavage reaction.

(b) The three-dimensional structure of the hammerhead ribozyme. The sequence of the hammerhead RNA used in this study and a three-dimensional schematic representation of its structure (Scott et al., 1995), showing the approximate spatial disposition of the bases in the orientation corresponding to Figures 3 and 5. This ribozyme construct employs a 16-nucleotide enzyme strand (green) and a 25-nucleotide substrate strand (blue and red). The letters outlined are absolutely or highly conserved bases in all hammerhead RNAs. The arrow denotes the self-cleavage site. The cleavage site nucleotide (C-17) and the adjacent nucleotide (A-1.1) of the substrate strand that are shown in Figure 1a are highlighted in red. The helices are labeled stem I, stem II, and stem III.

sequence but with a *tallo*-5'-C-methyl-ribose modification (Figure 1) designed to interfere with the final chemical step of the reaction, we have created a ribozyme that has an unaltered attacking nucleophile, but a modified leaving group that inhibits the actual cleavage event (Beigelman et al., 1995; L. B., unpublished data). The additional methyl group stabilizes the ordinarily scissile bond between the cleavage site phosphorus atom and the adjacent 5'-oxygen, presumably by altering the steric or electronic properties of this leaving group. We have employed this modified hammerhead RNA to capture a later conformational intermediate that is poised to form an in-line transition state. This structure provides us with a clearer and more detailed picture of how the hammerhead ribozyme works.

Results

A Modification of the Active Site that Slows Bond Cleavage

Modification of the hammerhead ribozyme active site by replacing the ribose leaving group with *tallo*-5'-C-methyl-ribose on residue 1.1 (Figure 1) slows the reaction at the point of bond scission. The rate of substrate turnover in the crystal with this modification is reduced well over 300-fold (Figure 2) relative to the cleavage rate in crystals of the corresponding unmodified hammerhead RNA under these conditions. In the presence of 50 mM CoCl₂ at pH 8.5, the cleavage rate of the unmodified hammerhead RNA in the crystal is approximately 0.4/min: 5-fold faster than in solution under these conditions and 10-fold faster than under "standard" reaction

conditions at pH 8.5. This 300-fold slower cleavage rate in the crystal suggests that the use of this modified ribozyme will allow reaction intermediates that occur

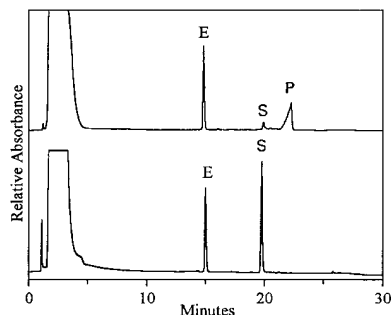


Figure 2. Hammerhead Ribozyme Cleavage in the Crystal

HPLC chromatograms showing almost complete cleavage of the unmodified hammerhead RNA after 4 min of soaking the crystal in 50 mM CoCl₂ artificial mother liquor as described in the Experimental Procedures (top trace) and no detectable cleavage in the 5'-C-methyl-A-1.1 modified hammerhead RNA crystals after 2.5 hr of soaking under the same conditions (bottom trace). The enzyme strand (E) elutes in 15 min, the uncleaved substrate strand (S) elutes just before 20 min, and the 20-mer cleavage product (P) elutes in 25 min. The 5-mer product cannot be detected using these conditions. Cleavage of the unmodified RNA in the crystal was virtually complete within 5 min; a time course within this range indicated an approximate turnover rate in the crystal of 0.4/min ± 0.1/min. In solution under otherwise identical conditions, the turnover rate was determined to be 0.08/min ± 0.01/min for the unmodified RNA sequence used for crystallization. Under standard reaction conditions (10 mM MgCl₂, 50 mM Tris at pH 8.5), the turnover rate for this construct is 0.04/min ± 0.01/min.

Table 1. Data Collection and Crystallographic Refinement

Experiment	100 mM CoCl ₂ 30 min Soak (pH 6) (Control 1)	50 mM CoCl ₂ 30 min Soak (pH 8.5) (Control 2)	50 mM CoCl ₂ 2.5 hr Soak (pH 8.5) (Conf. Change)	100 mM ZnCl ₂ 30 min Soak (pH 6)	100 mM CdCl ₂ 30 min Soak (pH 6)
Data collection					
X-ray source	Brookhaven X-12C	Brookhaven X-12C	Brookhaven X-12C	Brookhaven X-12C	Brookhaven X-12C
Wavelength (Å)	1.2700	1.2700	1.2700	1.2700	1.2700
Resolution (Å)	30–3.0	30–3.0	30–3.0	30–2.75	30–3.0
Completeness					
Overall	99.2%	85.2%	91.6%	94.8%	82.6%
(High res. bin)	(100%)	(78.8%)	(75.1%)	(85.9%)	(83.6%)
I/σ(I)					
Overall	34.71	19.98	12.6	24.33	21.43
(High res. bin)	(9.94)	(3.6)	(5.8)	(2.01)	(5.34)
R _{scale}					
Overall	0.052	0.061	0.046	0.074	0.064
(High res. bin)	(0.293)	(0.197)	(0.123)	(0.337)	(0.195)
Cell (a, c in Å)	65.15, 137.07	65.38, 138.15	65.10, 138.70	65.10, 136.85	64.95, 136.48
Refinement					
R factor (F > 2)	0.260	0.226	0.249 ^a	0.251	0.242
R free (10% data)	0.301	0.281	0.290 ^a	0.287	0.288
Geometry					
rmsd bonds (Å)	0.010	0.012	0.010	0.010	0.014
rmsd angles (°)	1.645	1.644	1.778	1.579	1.842
rmsd torsion angles (°)	15.600	17.797	19.899	16.970	17.947
rmsd planarity (°)	1.972	2.127	2.028	1.902	2.410

The five crystallographic trapping experiments performed are listed in columns, with conditions pertaining to each described in the title. Data collection and refinement statistics for each experiment are provided.

$R_{scale} = \frac{\sum |I_i - \langle I_i \rangle|}{\sum I_i}$ where I_i is the intensity value of an individual measurement and $\langle I_i \rangle$ is the corresponding mean value. Summations run over i measurements of all imaging plates.

R factor = $\frac{\sum |F_{obs} - F_{calc}|}{\sum |F_{obs}|}$.

R_{free} is the cross-validation R factor computed for the test set of reflections (10% of total).

^a The scissile phosphate atoms P and OP1 and OP2 of A-1.1 were omitted from refinement. When included as a pentacoordinated geometry, R factor = 0.247 and R_{free} = 0.289.

prior to bond breakage to accumulate at high occupancy in the crystal under appropriate cleavage conditions.

The Modified Leaving Group Does Not Change the Ground State or Early-Intermediate Structures

We tested the effect of the leaving group modification upon the initiation of the hammerhead ribozyme cleavage reaction in the crystal. We did so by comparing the crystal structures of the ground state and early intermediate determined previously for the unmodified ribozyme (Scott et al., 1996) with the corresponding ground state and early-intermediate crystal structures of the hammerhead ribozyme containing the 5'-C-methyl-ribose at the cleavage site.

Our preliminary experiments using the modified hammerhead RNA crystals at a cleavage-active pH (8.5) indicated that crystals soaked in 50 mM CoCl₂ (a divalent metal ion slightly more catalytically active than Mg²⁺) survived for several hours under otherwise identical conditions to those employed in crystal cleavage experiments previously (Scott et al., 1996). We therefore collected data on ground state crystals (control 1 in Table 1) of the modified RNA (\pm 100 mM CoCl₂) as well as on crystals soaked in an artificial mother liquor containing 50 mM CoCl₂ buffered at pH 8.5 for 30 min (control 2 in Table 2).

The ground state structure (both in the absence and presence of Co²⁺ at pH 6) was indistinguishable from the

isomorphous unmodified hammerhead RNA structure reported previously (Scott et al., 1996), and the structure of the (pH 8.5) Co²⁺-soaked hammerhead RNA after 30 min was essentially identical to the conformation observed in previous Mg²⁺ soaking experiments at pH 8.5 (Scott et al., 1996). These two structures therefore serve as controls (numbers 1 and 2 in Table 1) that prove that the presence of the extra methyl group does not disrupt the structures of the ground state or early cleavage intermediates of the hammerhead ribozyme, permitting us to argue that the added methyl group does not perturb significantly the initiation step of the reaction.

Capturing a Major Conformational Change at the Cleavage Site

Although the leaving group-modified RNA has the same ground state and early-intermediate structures as observed for the unmodified RNA, the modified RNA subsequently enabled us to capture a later and more informative intermediate structure in the course of the cleavage reaction. After 2.5 hr, the flash-frozen crystal of hammerhead RNA soaked in Co²⁺ revealed *further and more extensive* conformational changes in the positions of C-17 and the scissile phosphate of A-1.1 as shown in Figures 3a–3c. The base and ribose of C-17 have rotated about 60° in such a way as to cause the base of C-17 to move over 8.7 Å (as measured by the C-17 exocyclic nitrogen positions) to stack upon A-6

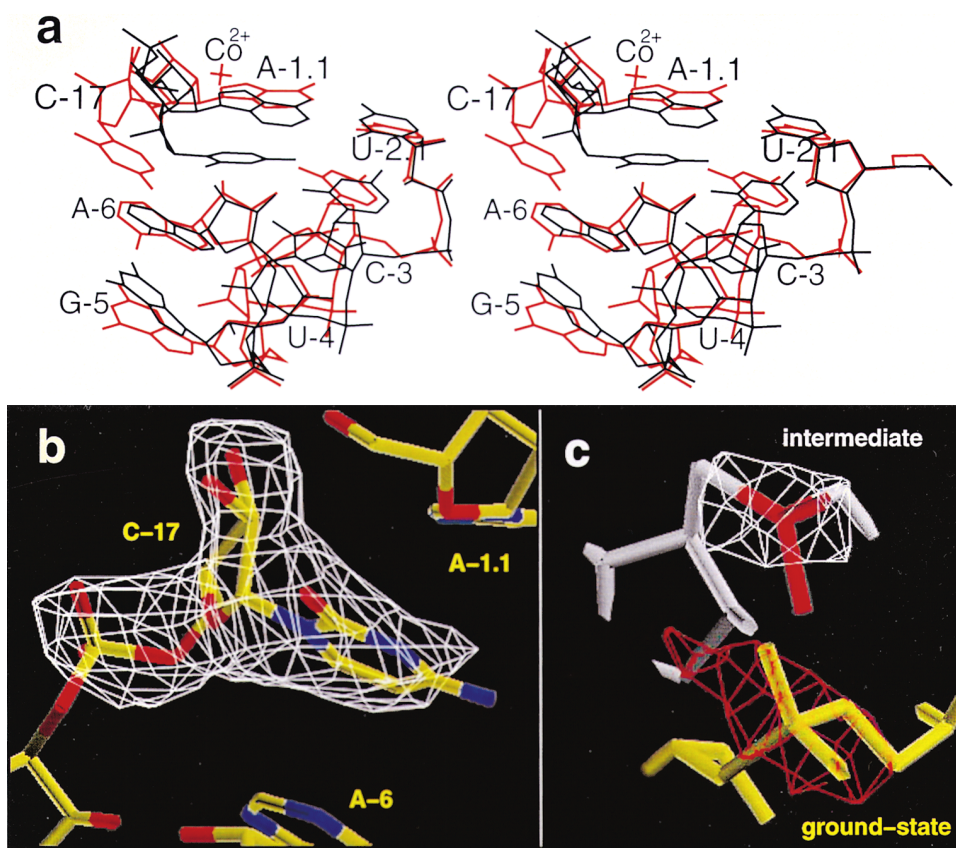


Figure 3. Conformational Changes that Activate Ribozyme Catalysis

(a) Stereo view of the hammerhead RNA catalytic pocket and first base pair (A-1.1 and U-2.1) of stem I, showing a superposition of the 2.5 hr (red) and 0.5 hr (black; control 2 in Table 1) high pH Co(II) freeze-trapped structures. Note the major conformational change of the cleavage site base (C-17) as it swings out to stack upon A-6, which is in turn stacked upon G-5. The conformation of G-5 also changes to a smaller extent. The scissile phosphate has been omitted from this stage of the refinement (see text).

(b) A simulated annealing omit difference Fourier ($F_{\text{obs}} - F_{\text{calc}}$) map contoured at 3σ (in white) showing clear difference density for the new position of C-17. The base and scissile phosphate were omitted from a refinement starting with the ground state structure, as described in the Experimental Procedures. The kinetically trapped conformational intermediate model is superimposed upon the electron density for clarity of interpretation.

(c) The experimentally observed amplitudes for the late-intermediate structure can be compared directly to the experimentally observed amplitudes of the ground state structure without introducing any model bias for the new position of the phosphate by construction of an isomorphous difference Fourier electron density map having coefficients of the form $[F_{\text{obs}}(\text{late-intermediate}) - F_{\text{obs}}(\text{ground state})]$ and phases calculated solely from the ground state structure. The positive difference Fourier peak at 3σ , shown in white, indicates the position of the phosphate in the late-intermediate structure. The analogous $[F_{\text{obs}}(\text{ground state}) - F_{\text{obs}}(\text{late-intermediate})]$ map shows a "negative" density peak at 3σ , in red, indicating the vacated initial position of the phosphate relative to the ground state structure.

(which remains stacked upon G-5). Additionally, the furanose oxygen of A-1.1 now stacks upon the base of C-17, and therefore the entire platform of C-17, A-6, and G-5. Movement of the cleavage site base has the effect of inducing a conformational change in the scissile phosphate, pulling the phosphate away from its original standard helical geometry, as shown by the difference Fourier peak for this new phosphate position in Figure 3c. This effect is addressed in the Discussion.

In addition to the major rearrangement of C-17 (and some rotational disorder observed for U-4 in the catalytic pocket of the kinetically trapped hammerhead ribozyme, as seen in Figure 3a), several other changes take place at locations more distant to the cleavage site. The most significant of these is at the junction between stem III and the augmented stem II helix (or domain II) where U-16.1 rotates approximately 70° about the glycosyl

bond relative to the ground state structures, creating an "edge-to-face" stacking interaction with U-7. Other changes include distortion of the A-13–G-8 base pair in such a way that hydrogen bonds between the bases can no longer form (although the interstrand stacking is preserved), and the phosphate of A-9 changes conformation in such a way as to alter potentially its metal-binding environment. It is likely that these more distant conformational changes are induced by those observed near the catalytic pocket, or vice versa.

Verification of the Observed Conformational Changes at the Cleavage Site

The validity of the conformational changes in C-17 and the adjacent scissile phosphate were checked using a variety of simulated annealing omit difference Fourier procedures. These tests reveal unambiguous difference

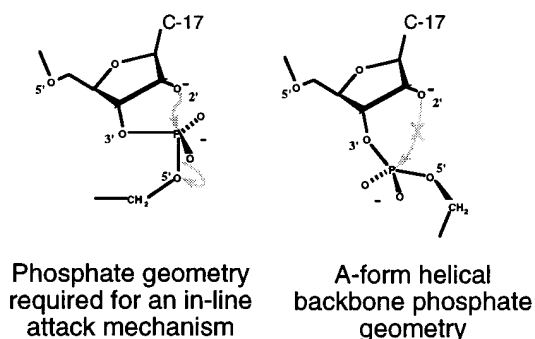


Figure 4. The Cleavage Site Phosphate Conformational Switch

A schematic diagram illustrating the fact that a helical phosphate conformation is maximally incompatible with (i.e., 90° away from) the conformation required for an in-line attack mechanism. Therefore, any significant movement away from the helical phosphate conformation will bring it closer to the geometry required for in-line attack. Such a change in the scissile phosphate is required by the observed conformational change of C-17 shown in Figures 3a and 3b.

electron density for the new position of the base and ribose of C-17 (Figure 3b) and of the scissile phosphate (Figure 3c) in the kinetically trapped intermediate structure.

Initially, to verify the conformational changes, both C-17 and the adjacent scissile phosphate (the phosphorus and nonbridging oxygens of A-1.1) were omitted from a simulated annealing molecular dynamics refinement of the “late”-intermediate data set, using the ground state crystal structure as the starting point for the refinement. Both the resulting omit- $(2F_{\text{obs}} - F_{\text{calc}})$ and omit- $(F_{\text{obs}} - F_{\text{calc}})$ maps (Figure 3b) clearly reveal the position of the nucleotide base and ribose of C-17. These parts of the model were then included for a subsequent refinement, in which the phosphorus and nonbridging oxygens of A-1.1 were again omitted.

The position of the omitted scissile phosphorus atom was subsequently deduced on the basis of both $(F_{\text{obs}} - F_{\text{calc}})$ and $(F_{\text{obs}}^+ - F_{\text{obs}}^-)$ difference Fouriers and then confirmed with two separate $[F_{\text{obs}}(\text{late-intermediate}) - F_{\text{obs}}(\text{ground state})]$ isomorphous difference Fouriers, using phases calculated with the ground state structure (Figure 3c). The latter difference Fourier confirms the scissile phosphate conformational change without model bias and has the additional merit of revealing negative difference density corresponding to the ground state phosphorus location.

Discussion

The Ground State Hammerhead RNA Structures Do Not Reveal the Cleavage Mechanism

The ground state structures revealed the architectural principles of hammerhead ribozyme folding (Pley et al., 1994; Scott et al., 1995) and hinted at a possible catalytic mechanism (Scott et al., 1995). In each ground state structure, however, the cleavage site phosphate was found to be in the standard helical phosphate conformation. This conformation is maximally (or 90°) out of register for an in-line attack cleavage mechanism, as is

shown schematically in Figure 4. Therefore, a very serious objection was raised: How does the structure of the hammerhead ribozyme activate scissile bond cleavage if the scissile phosphate is in a conformation maximally incompatible with the orientation required by the known chemical mechanism? The structural basis of hammerhead ribozyme self-cleavage therefore cannot be addressed merely by examining the ground state structures of the ribozyme. Because of this, we have attempted to understand hammerhead ribozyme catalysis using techniques of time-resolved crystallography that have proven successful for capturing protein enzyme intermediates. The results of our investigation, as reported here, are discussed below.

The Effect of the C-17 Rearrangement upon the Scissile Phosphate in the Kinetically Trapped Intermediate Conformation

The 60° rotation of the base of C-17 with respect to the ground state structure, combined with the concomitant conformational change of the C-17 ribose that flips the 2'-OH upward toward the scissile phosphate (Figure 3a), has the effect of preventing the scissile phosphate from adopting the standard helical conformation that is found in all of the ground state hammerhead RNA crystal structures, due to the geometrical restrictions created by the movement of the cleavage site base and ribose. For this reason, the scissile phosphate was omitted from the initial refinement of the structures shown in Figures 3b and 3c. This result is especially intriguing in light of the fact that the original helical phosphate conformation was incompatible with an in-line attack cleavage mechanism, as summarized in Figure 4. (The helical phosphate conformation accounts for the relative stability of helical RNA compared to nonhelical regions.) Therefore, any conformational change in the phosphate that causes it to deviate significantly from the helical conformation will be more susceptible to in-line attack, as shown in Figure 4. The effect of the C-17 conformational change is therefore to perturb the helical conformation of the scissile phosphate, thus rendering it more susceptible to nucleophilic attack from the cleavage site 2'-hydroxyl, also repositioned by the conformational change.

The Catalytic Relevance of the Intermediate Conformation

The phosphate conformation of the kinetically trapped intermediate structure must be close to that inhabited by the chemical intermediate or transition state of the cleavage reaction, as may be seen by examining the phosphate position dictated by the difference Fourier peak shown in Figure 3c. The position of the phosphorus atom is compatible with the geometry required by an in-line attack mechanism, although specific details of the nonbridging phosphate oxygen positions cannot be resolved unambiguously at 3 Å resolution, as is apparent from Figure 3c.

To find the intermediate structure most compatible with the experimental observations without overfitting the data, the structure was variously refined using a 2',3'-cyclic diester phosphate, a 2',3',5'-triestor oxyphosphorane (based on the known geometry of a vanadium transition state analog in which the vanadium is

replaced by phosphorus for the purpose of modeling), and with a standard A form 3',5'-phosphate. Although the first two structures were compatible with the observed electron density and the remainder of the kinetically trapped RNA structure (Figure 3), the standard helical phosphate was not compatible with either the observed electron density or the remainder of the RNA structure. Gel electrophoresis and HPLC analyses of identically treated crystals reveal that the crystallized RNA has not been cleaved, ruling out the 2',3'-cyclic phosphate as the most accurate model (Figure 2).

The pentacoordinated phosphate intermediate or transition state model is consistent with the kinetically trapped late conformational intermediate (Figure 5). Although the observed electron density (Figure 3c) is compatible with the modeled oxyphosphorane intermediate model, such a structure cannot be resolved unambiguously with a 3 Å resolution electron density map. It is indeed extremely unlikely that an evanescent pentacoordinated phosphate intermediate structure could in fact be captured using these techniques. The structure shown in Figure 5 demonstrates that the conformation of the phosphate is geometrically compatible with future formation of such an intermediate or transition state. The safest interpretation is therefore that the scissile phosphate, though uncleaved, is no longer anywhere near to the ground state conformation that is maximally incompatible with in-line attack and has therefore been activated by the unambiguous 60° rotation and 8.7 Å translation observed for C-17.

Conservation of Stacking Interactions in the Catalytic Pocket

The catalytic pocket conformation changes in such a way as to preserve the connectivity of stacking interactions as shown in Figures 5a and 5b. In the ground state structure, the base of C-17 stacks upon A-1.1 of stem I, and the furanose oxygen of C-17 stacks upon A-6 of the catalytic pocket, which in turn stacks upon G-5. Stacking in the hammerhead RNA ground state structure, in fact, involves every base except U-4 and U-7. The kinetically trapped conformational intermediate structure (Figure 5), though the product of a large-scale movement of C-17, preserves the catalytic pocket stacking connectivity. Although the base of C-17 no longer stacks upon stem I, it now stacks upon A-6, which remains stacked to G-5. It is now the furanose oxygen of A-1.1 that stacks upon the base of C-17, thus preserving the overall connectivity of these stacking interactions as shown in Figure 5b. The energetics of stacking interactions contributes significantly to stabilizing RNA tertiary structure; therefore, it is not surprising that a conformational change in the hammerhead RNA structure would be constrained in such a way as to conserve stacking contacts as much as possible. We suggest that conservation of stacking connectivity may be a general rule that governs which RNA conformational changes will be physically allowed.

Positioning of Metal Ions near G-5 and the Leaving Group 5'-Oxygen

Crystals soaked separately in 100 mM Co^{2+} , Zn^{2+} , and Cd^{2+} at pH 6 reveal two sets of metal-binding sites

located near G-5, a highly conserved residue of the hammerhead ribozyme catalytic pocket. Common to all three is a site approximately 2.5 Å from N7 of G-5. Co^{2+} and Zn^{2+} share a second, apparently outer-sphere coordination to the exocyclic groups of G-5. (This site is also occupied by Mn^{2+} and Tb^{3+} ; see Scott et al., 1996; Feig et al., 1998). However, Cd^{2+} binds with a slightly different geometry, making apparent outer-shell contacts with both G-5 and A-6, placing it closer to the cleavage site ribose.

As well as the observed conformational change, the 2.5 hr Co^{2+} soaking experiment revealed one remaining Co^{2+} ion located 2.5 Å from N7 of G-5 as well as clear difference density for a new Co^{2+} ion located 2.3 Å from N7 of A-1.1 and near the 5'-oxygen leaving group. The position of the Co^{2+} ion near the scissile phosphate is similar to a Mg^{2+} position observed previously (Scott et al., 1996), with the exception that the Mg^{2+} appeared to make an inner-sphere contact with the *pro-R* oxygen of the scissile phosphate and an outer-sphere contact with N7 of A-1.1. Here, Co^{2+} makes an inner-sphere contact to A-1.1. This difference may be a function of the hardness (Pearson, 1963) of Mg^{2+} versus Co^{2+} or perhaps the somewhat different conformations of the RNA. In any case, this divalent metal ion appears to interact with the leaving group 5'-oxygen of A-1.1, possibly serving as a general acid catalyst by donating a proton from an inner-sphere coordinated water molecule (Steitz and Steitz, 1993; Uchimarui et al., 1993). Replacement of A-1.1 with U leads to an approximate 10-fold increase in hammerhead activity, suggesting that the geometry imposed by direct chelation of a metal ion to the N7 of A-1.1 may be suboptimal (Clouet-Dorval and Uhlenbeck, 1996).

Concluding Remarks

The cleavage mechanism that we have extrapolated from our experimental results postulates that the most dramatic conformational changes that occur during the cleavage reaction are local, being restricted to C-17, the backbone of A-1.1, and to a lesser extent, the uridine turn and other conserved regions of the hammerhead ribozyme. Although it may be possible that the crystal lattice contacts restrain the RNA from making more global conformational changes during and especially after cleavage (Peracchi et al., 1997), it must be noted that these crystallographically unobservable global changes would have to be compatible with the results of cross-linking experiments that are consistent with the ground state (crystal) structure of the hammerhead ribozyme and inconsistent with most major conformational rearrangements (Sigurdsson et al., 1995). Furthermore, results of transient electric birefringence (Amiri and Hagerman, 1996) and gel electrophoresis experiments (Bassi et al., 1996, 1997) also suggest lack of a global conformational change during cleavage. Recent NMR evidence does, however, suggest an interaction between U-4 and U-7 in the cleaved structure of the hammerhead RNA (Simorre et al., 1997), indicating more conformational plasticity ("floppiness") in the cleaved structure (Hertel et al., 1994) than that observed in the fold of

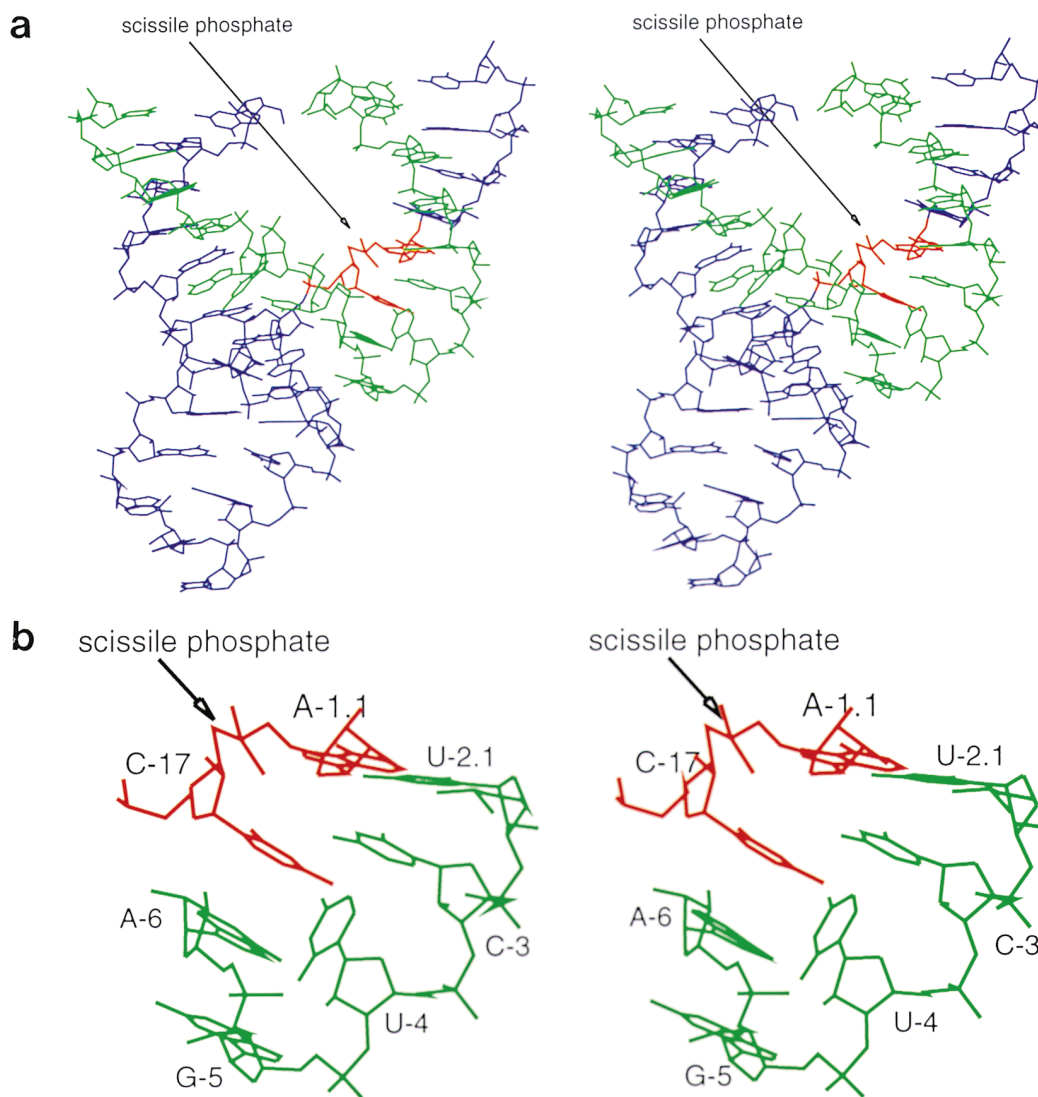


Figure 5. Stereo Views of the Kinetically Trapped Hammerhead Ribozyme Late-Intermediate Structure

(a) Stereo view of the entire kinetically trapped late-conformational-intermediate structure, with the scissile phosphate indicated. The color scheme follows Figure 1b. The position of the scissile phosphate is based upon the difference Fourier peak shown in Figure 3c.

(b) Close up stereo view of the catalytic pocket, with residues labeled. Note the position of C-17. The scissile phosphate is shown as having a geometry compatible with the observed requirement for an in-line attack mechanism and further restrained by the position of the phosphorus difference Fourier peak (shown in Figure 3c).

uncleaved or cleaving hammerhead ribozymes. Finally, it is worth noting that analogous conformational changes in the cleavage site ribose of the hammerhead RNA have been predicted in molecular dynamics simulations of ribozyme cleavage that start with our ground state structure (Herman et al., 1997, 1998).

Experimental Procedures

Crystallization and Data Collection

The use of chemically synthesized RNA (Wincott et al., 1995) was essential to incorporate specifically the modified nucleotide into crystals of the hammerhead ribozyme. We grew the crystals using established conditions (Scott et al., 1996) from 1 mM hammerhead RNA in 1.8 M Li_2SO_4 , 50 mM sodium cacodylate (pH 6) and 1.5 mM

EDTA (final concentrations). The crystals grew within 24 hr in space group P3₁21 with cell dimensions approximately $a = 65 \pm 0.5 \text{ \AA}$, $c = 136 \pm 1.5 \text{ \AA}$ (depending upon experimental soaking conditions) and diffracted to 3 Å (with the exception of crystals soaked in Zn^{2+} , which diffracted to 2.7 Å) when maintained at 100 K. The crystals were soaked in an artificial mother liquor containing 1.8 M Li_2SO_4 , 50 mM buffer (either cacodylate buffer at pH 6 or Tris buffer at pH 8.5 as indicated in the first row of Table 1) and augmented by the divalent metal ion listed in the first row of Table 1, as well as 20% glycerol. The crystals were soaked for the indicated time period and then flash-frozen in liquid nitrogen and maintained at 100 K with an Oxford Cryosystems nitrogen cooling system. Synchrotron data were collected at Brookhaven beamline X12C using a custom-built CCD detector as indicated in Table 1. The data were processed using Denzo (Otwinowski and Minor, 1997) as well as the CCP4 crystallographic computing package (CCP4, 1994).

Refinement of Structures

The structures were refined using X-PLOR 3.1 (Brünger, 1993), employing ideal nucleic acid parameters (Parkinson et al., 1996) weighted against the observed electron density. The previously published crystal structure of an unmodified ground state hammerhead RNA of identical sequence and crystal form (Scott et al., 1996) was used as a starting model for all of the refinements. The model building was performed using the graphics display program O (Jones and Kjeldgaard, 1997), from which Figures 3 and 5 were made. The crystal structure of the conformational intermediate was similarly refined in X-PLOR, initially omitting the phosphorus and the two nonbridging phosphate oxygens from the refinement in order to avoid model biasing. Upon completion of this refinement, it appeared that a large-scale conformational change in C-17 had taken place. The new conformation of C-17 was confirmed by repeating the refinement using three different simulated annealing trajectories while omitting C-17 and the scissile phosphate from the calculation, again using the ground state structure as a starting model for the refinement. A representative simulated annealing omit map (Read, 1986; Hodel et al., 1992) is shown in Figure 3b, revealing clear difference density for the new position of C-17.

Modeling the Scissile Phosphate of the Kinetic Intermediate

Finally, the scissile phosphate was modeled using, in turn, a 2',3'-cyclic phosphate diester, a 2',3',5'-oxyphosphorane triester based on the trigonal bipyramidal geometry of a vanadium analog, and a standard helical 3',5'-phosphate diester geometry. The first two models refined without problem; the standard helical phosphodiester, however, could not be forced into the observed electron density in a manner compatible with the rest of the conformationally changed structure. The final structure reported again omits the three phosphate atoms in question in order to eliminate the possibility of biasing the structure with our interpretation of the cleavage site phosphate geometry.

Crystal Cleavage Assay

We assayed the cleavage in the crystal by gel electrophoresis and HPLC, the latter method proving more versatile for the high-salt conditions employed. We soaked the crystals in the pH 8.5 reaction mixture (50 mM CoCl₂, 1.8 M Li₂SO₄, 20% glycerol, and 50 mM Tris buffer) for various periods of time. Instead of flash freezing a crystal of either the modified or unmodified hammerhead ribozyme to arrest cleavage, the chosen crystal was instead removed with a rayon loop from the cleavage reaction conditions after a predetermined time and immersed immediately into 50 μ l of 0.5 M EDTA and allowed to soak for 30 min before dissolving it in the EDTA solution. The sample was then analyzed at 50°C by ion-exchange HPLC, (Dionex DNA-PAC) using a gradient of 350 mM to 650 mM NH₄Cl in 22 min. Representative chromatograms are shown in Figure 2.

Acknowledgments

We thank Aaron Klug, Stephen Price, Barry Stoddard, and Robert Sweet for help and advice.

Received December 11, 1997; revised January 26, 1998.

References

Amiri, K.M., and Hagerman, P. (1996). The global conformation of an active hammerhead RNA during the process of self-cleavage. *J. Mol. Biol.* **261**, 125–134.

Bassi, G.S., Murchie, A.I.H., and Lilley, D.M.J. (1996). The ion-induced folding of the hammerhead ribozyme: core sequence changes that perturb folding into the active conformation. *RNA* **2**, 756–768.

Bassi, G.S., Murchie, A.I.H., Walter, F., Clegg, R.M., and Lilley, D.M.J. (1997). Ion-induced folding of the hammerhead ribozyme: a fluorescence resonance energy transfer study. *EMBO J.* **16**, 7481–7489.

Beigelman, L., Karpeisky, A., and Usman, N. (1995). Synthesis of

5'-C-methyl-D-allo- and L-tallo-ribonucleoside 3'-O-phosphoramidites and their incorporation into hammerhead ribozymes. *Nucleosides Nucleotides* **14**, 901–905.

Bolduc, J.M., Dyer, D.H., Scott, W.G., Singer, P., Sweet, R.M., Koshland, Jr., D.E., and Stoddard, B.L. (1995). Mutagenesis and laue structures of enzyme intermediates: isocitrate dehydrogenase. *Science* **268**, 1312–1317.

Brown, R.S., Dewan, J.C., and Klug, A. (1985). Crystallographic and biochemical investigation of the lead(II)-catalyzed hydrolysis of yeast phenylalanine tRNA. *Biochemistry* **24**, 4785–4801.

Brünger, A.T. (1993). X-PLOR 3.1: A System for Crystallography and NMR (New Haven, CT: Yale University Press).

Clouet-Dorval, B., and Uhlenbeck, O.C. (1996). Kinetic characterization of two I/II format hammerhead ribozymes. *RNA* **2**, 483–491.

Collaborative Computational Project, Number 4 (CCP4) (1994). The CCP4 suite: programs for protein crystallography. *Acta Crystallogr. D50*, 760–763.

Dahm, S., and Uhlenbeck, O.C. (1991). Role of divalent metal ions in the hammerhead RNA cleavage reaction. *Biochemistry* **30**, 9464–9469.

Dahm, S., Derrick, W.B., and Uhlenbeck, O.C. (1993). Evidence for the role of solvated metal hydroxide in the hammerhead cleavage mechanism. *Biochemistry* **32**, 13040–13045.

Feig, A., Scott, W.G., and Uhlenbeck, O.C. (1998). Inhibition of the hammerhead ribozyme cleavage reaction by site-specific binding of Tb(III). *Science* **279**, 81–84.

Guerrier-Takada, C., Gardiner, K., Marsh, T., Pace, N., and Altman, S. (1983). The RNA moiety of ribonuclease P is the catalytic subunit of the enzyme. *Cell* **35**, 849–857.

Herman, T., Auffinger, P., Scott, W.G., and Westhof, E. (1997). Evidence for a hydroxide ion bridging two magnesium ions at the active site of the hammerhead ribozyme. *Nucleic Acids Res.* **25**, 3421–3427.

Herman, T., Auffinger, P., and Westhof, E. (1998). Molecular dynamics investigations on the hammerhead ribozyme RNA. *Eur. J. Biophys.*, in press.

Hertel, K.J., Herschlag, D., and Uhlenbeck, O.C. (1994). A kinetic and thermodynamic framework for the hammerhead ribozyme reaction. *Biochemistry* **33**, 3374–3385.

Hodel, A., Kim, S.-H., and Brünger, A.T. (1992). Model bias in macromolecular crystal structures. *Acta Crystallogr.* **A48**, 851–859.

Jones, T.A., and Kjeldgaard, M. (1997). *O* Version 6.1.0 (Dept. of Mol. Biol., BMC, Uppsala Univ., Sweden, and Dept. of Chem., Aarhus Univ., Denmark).

Koizumi, M., and Ohtsuka, E. (1991). Effects of phosphorothioate and 2-amino groups in hammerhead ribozymes on cleavage rates and Mg²⁺ binding. *Biochemistry* **30**, 5145–5150.

McKay, D.B. (1996). Structure and function of the hammerhead ribozyme: an unfinished story. *RNA* **2**, 395–403.

Moffat, K., and Henderson, R. (1995). Freeze-trapping of reaction intermediates. *Curr. Opin. Struct. Biol.* **5**, 656–661.

Otwinowski, Z., and Minor, W. (1997). Processing of X-ray diffraction data collected in oscillation mode. *Methods Enzymol.* **276**, 307–326.

Parkinson, G., Vojtechovsky, J., Clowney, L., Brünger, A.T., and Berman, H.M. (1996). New parameters for the refinement of nucleic acid-containing structures. *Acta Crystallogr.* **D52**, 57–69.

Pearson, R.G. (1963). Hard and soft acids and bases. *J. Am. Chem. Soc.* **85**, 3533–3539.

Peracchi, A., Beigelman, L., Scott, E.C., Uhlenbeck, O.C., and Herschlag, D. (1997). Involvement of a specific metal ion in the transition of the hammerhead ribozyme to its catalytic conformation. *J. Biol. Chem.* **272**, 26822–26826.

Pley, H.W., Flaherty, K.M., and McKay, D.B. (1994). Three-dimensional structure of a hammerhead ribozyme. *Nature* **372**, 68–74.

Read, R.J. (1986). Improved Fourier coefficients for maps using phases from partial structures with errors. *Acta Crystallogr.* **A42**, 140–149.

Scott, W.G., and Klug, A. (1996). Ribozymes: structure and mechanism in RNA catalysis. *Trends Biochem. Sci.* **21**, 220–224.

Scott, W.G., Finch, J.T., and Klug, A. (1995). The crystal structure of an all-RNA hammerhead ribozyme: a proposed mechanism for RNA catalytic cleavage. *Cell* *81*, 991–1002.

Scott, W.G., Murray, J.B., Arnold, J.R.P., Stoddard, B.L., and Klug, A. (1996). Capturing the structure of a catalytic RNA intermediate: the hammerhead ribozyme. *Science* *274*, 2065–2069.

Sigurdsson, S.-T., Tuschl, T., and Eckstein, F. (1995). Probing RNA tertiary structure: interhelical crosslinking of the hammerhead ribozyme. *RNA* *1*, 575–583.

Simorre, J.-P., Legault, P., Hangar, A.B., Michiels, P., and Pardi, A. (1997). A conformational change in the catalytic core of the hammerhead ribozyme upon cleavage of an RNA substrate. *Biochemistry* *36*, 518–525.

Slim, G., and Gait, M.J. (1991). Configurationally defined phosphorothioate-containing oligoribonucleotides in the study of the mechanism of cleavage of hammerhead ribozymes. *Nucleic Acids Res.* *19*, 1183–1188.

Steitz, T.A., and Steitz, J.A. (1993). A general two-metal-ion mechanism for catalytic RNA. *Proc. Natl. Acad. Sci. USA* *90*, 6498–6502.

Symons, R.H. (1992). Small catalytic RNAs. *Annu. Rev. Biochem.* *61*, 641–671.

Thomson, J.B., Tuschl, T., and Eckstein, F. (1996). The hammerhead ribozyme. In *Nucleic Acids and Molecular Biology*, Vol 10., F. Eckstein and D.M.J. Lilley, eds. (Berlin: Springer-Verlag), pp. 173–196.

Uchimaru, T., Tanabe, K., Shimayama, T., Uebayasi, M., and Taira, K. (1993). Theoretical analyses on the role of metal cations in RNA cleavage processes. *Nucleic Acids Symp. Ser.* *29*, 179–180.

Uhlenbeck, O.C. (1987). A small catalytic oligoribonucleotide. *Nature* *328*, 596–600.

van Tol, H., Buzayan, J.M., Feldstein, P.A., Eckstein, F., and Bruening, G. (1990). Two autolytic processing reactions of a satellite RNA proceed with inversion of configuration. *Nucleic Acids Res.* *18*, 1971–1975.

Wincott, F., DiRenzo, A., Shaffer, C., Grimm, S., Tracz, D., Workman, C., Sweedler, D., Gonzalez, C., Scaringe, S., and Usman, N. (1995). Synthesis, deprotection, analysis and purification of RNA and ribozymes. *Nucleic Acids Res.* *23*, 2677–2684.

Zaug, A.J., and Cech, T.R. (1986). The intervening sequence RNA of *Tetrahymena* is an enzyme. *Science* *231*, 470–475.

Nucleic Acid Database Accession Numbers

The accession number for the coordinates of structures reported in this paper is URX071, and for the original ground state structure is URX057.